Vol 18 No 9, September 2009
1674-1056/2009/18(09)/3687-06

Chinese Physics B

© 2009 Chin. Phys. Soc.
and IOP Publishing Ltd

Enhancement of next-nearest-neighbouring entanglement in quantum Ising spin chain*

Shan Chuan-Jia(单传家)†, Liu Ji-Bing(刘继兵), Cheng Wei-Wen(程维文), Liu Tang-Kun(刘堂昆), Huang Yan-Xia(黄燕霞), and Li Hong(李 宏)

College of Physics and Electronic Science, Hubei Normal University, Huangshi 435002, *China*

(Received 28 February 2009; revised manuscript received 19 March 2009)

Using the method of the Jordan–Wigner transformation for solving different spin–spin correlation functions, we have investigated the generation of next-nearest-neighbouring entanglement in a one-dimensional quantum Ising spin chain with the Gaussian distribution impurities of exchange couplings and external magnetic fields taken into account. The maximal value of entanglement between the next-nearest-neighbouring qubits in the transverse Ising model was analysed in detail by varying the effectively controlled parameters such as interchange coupling, magnetic field and the system impurity. For such systems, where both exchange couplings and external magnetic field disorder appear, we show that it is possible to achieve next-nearest-neighbouring entanglement better than the previously discussed pure Ising spin chain case. We also show that the Gaussian distribution impurity can induce next-nearest-neighbouring entanglement, which can be used as a means to characterize quantum phase transition.

Keywords: next-nearest-neighbouring entanglement, Ising spin chain, Jordan–Wigner transformation

PACC: 0365, 7510H

1. Introduction

Entanglement is one of the most fundamental and intriguing features of quantum mechanics and has practical applications in many quantum information processes (QIP), including quantum teleportation, quantum cryptography, quantum computers, etc.[1−4] Over the past few years, a large number of schemes have been proposed for generating entangled state in various quantum systems, which include semiconductor quantum dots, cavity quantum electrodynamics, trapped ions, and spin chain systems. Among these quantum systems, the spin system with Heisenberg exchange interaction deserves much attention and the entanglement properties have been extensively investigated in spin systems, such as the Ising model[5] and the isotropic and anisotropic Heisenberg models.[6−9] The entanglement in spin chains can be used in quantum information processing.[10] The reason for considering disordered systems for QIP is that potentially they could offer advantages for quantum information tasks compared to ordered systems. First, since they have typically a large number of different metastable free energy minima, such states might be used to store information distributed over the whole system, similarly to neural network models. Second, in disordered systems with long range interactions, the stored information is robust.

The one-dimensional (1D) transverse-field Ising model is one of the simplest models which can be solved exactly[11,12] in the field of condensed matter physics. Due to its simplicity and clear physical pictures, the model is often used as a starting one to test new physical ideas and approaches. Furthermore, the interest in the content of entanglement available in statistical systems has also increased due to the observed correction between entanglement and quantum critical phenomena. Quantum phase transition(QPT) in a many-body system, which occurs at absolute zero temperature and is purely driven by quantum fluctuations, is the structural change in the properties of the ground state. The associated level crossings lead to the presence of non-analyticities in the energy spectrum. Indeed, it has been noted that QPTs present in condensed matter systems can be described from the point of view of entanglement. As examples, many systems have been found where QPT is accompanied

*Project supported by the Foundation for Scientific and Technological Research Programme, Education Department of Hubei Province, China (Grant No Z200722001), and the Postgraduate Programme of Hubei Normal University of China (Grant No 2007D20).

†E-mail: scj1122@163.com

by a qualitative change of the entanglement, and the ground-state pairwise entanglement of XY and XXZ chains in a transverse magnetic field has been worked out,[13−17] from which scaling behaviour near the transition point is observed.

Recently, Osterloh *et al*[18] examined the entanglement between two spins of position i and j in the spin chains for the pure case, Huang *et al*,[19] Osenda *et al*[20] and we[21] have demonstrated that entanglement can be controlled and tuned by introducing impurities into the systems. As far as we know, most of the works focused on the entanglement between the nearest pairs by the effectively controlled factors such as temperature, interchange coupling, magnetic field and system impurity. However, there exists entanglement between the next-nearest-neighbour qubits in the transverse Ising model, but the maximal value of entanglement is only about 4.3×10^{-3}. Moreover, the maximum value of the concurrence between the next-nearest-neighbouring sites does occur at the critical point $\lambda = 1$, so it is necessary to discuss the effect on the next-nearest-neighbouring entanglement. Venuti *et al*[22,23] proposed a scheme with a nearest interaction (dimerization) and a uniform next nearest interaction to realize a long-distance entanglement in a spin system and further proposed to use it for teleportation and state transfer. In this article, we investigate how to create long distance entanglement in a 1D disordered Ising spin system. The disordered parameters increase the next-nearest-neighbouring entanglement, and the knowledge about the ground-state entanglement, the nonlocal correlation in quantum systems, is considered as a key to further understand QPT. So the Gaussian distribution impurity induced next-nearest-neighbouring entanglement, which can be used as a means to characterize the QPT. Our motivation is to find which parameters are crucial in creating the next-nearest-neighbouring entanglement between two qubits, and thus to simplify the model to control or manipulate the entanglement in a spin system with the help of exchange couplings, external magnetic fields and the system impurity.

2. Solution of the XY model and spin–spin correlation functions

The model we study is a physical Ising chain consisting of N spins with nearest-neighbouring interactions and an external magnetic field. In the presence of impurities, the Hamiltonian of the 1D transverse-field Ising model under periodic boundary conditions reads

$$H = \sum_{i=1}^{N} J_{i,i+1}\sigma_i^x\sigma_{i+1}^x - \sum_{i=1}^{N} h_i\sigma_i^z, \tag{1}$$

where $J_{i,i+1}$ is the exchange interaction between sites i and $i+1$, h_i is the strength of the external magnetic field on site i, $\sigma^{x,y,z}$ are the Pauli matrices, and N is the number of sites. Each site i is subjected to a magnetic field in the z direction, giving the energy splitting h_i. In this description, the excitation energy of a qubit is the Zeeman energy of a spin. In this disordered chain, not all the qubits have the same level spacing. The energy of two qubits, called defects, differs from those of other qubits. The periodic boundary conditions satisfy $\sigma_{N+1}^x = \sigma_1^x, \sigma_{N+1}^y = \sigma_1^y, \sigma_{N+1}^z = \sigma_1^z$.

A major advantage of the above Hamiltonian is that it can be diagonalized exactly. Let us briefly review the main steps of the diagonalization of H: the set of N qubits in Eq.(1) can be mapped to a system of N spinless fermions via the Jordan–Wigner transformation.[24] One defines the raising and lowering operators a_i^+, a_i^- and introduces Fermi operators[25] c_j^+, c_j,

$$a_i^+ = \frac{1}{2}(\sigma_i^x + \mathrm{i}\,\sigma_i^y) = c_i^+ \exp\left(\mathrm{i}\,\pi\sum_{j=1}^{i-1} c_j^+ c_j\right), \tag{2}$$

$$a_i^- = \frac{1}{2}(\sigma_i^x - \mathrm{i}\,\sigma_i^y) = \exp\left(-\mathrm{i}\,\pi\sum_{j=1}^{i-1} c_j^+ c_j\right) c_i. \tag{3}$$

So, the Hamiltonian (1) can be transformed into

$$H = -\sum_{i=1}^{N} J_{i,i+1}[(c_i^+ c_{i+1} + c_i^+ c_{i+1}^+) + h.c] - 2\sum_{i=1}^{N} h_i\left(c_i^+ c_i - \frac{1}{2}\right). \tag{4}$$

In this paper, the exchange interaction has the form $J_{i,i+1} = J(1+\alpha_{i,i+1})$, where α introduces the impurity in a Gaussian form centred at $\dfrac{N+1}{2}$ with strength ζ,

$$\alpha_{i,i+1} = \zeta \exp\left\{-\epsilon\left(i - \frac{N+1}{2}\right)\right\}. \tag{5}$$

The external magnetic field takes the form $h_i = h(1+\beta_i)$, where

$$\beta_i = \xi \exp\left\{-\epsilon\left(i - \frac{N+1}{2}\right)\right\}. \tag{6}$$

When $\alpha = \beta = 0$, we recover the pure Ising spin chain case. By introducing the dimensionless parameter $\lambda = J/2h$, the symmetrical matrix $\boldsymbol{A}$ and the antisymmetrical $\boldsymbol{B}$, the Hamiltonian becomes

$$H = \sum_{i,j=1}^{N} \left[c_i^+ A_{i,j} c_j + \frac{1}{2}(c_i^+ B_{i,j} c_j^+ + \text{h.c}) \right]. \tag{7}$$

The above Hamiltonian can be diagonalized by making linear transformation of the fermionic operators $\eta_k = \sum_{i=1}^{N} g_{ki} c_i + h_{ki} c_i^+$, and $\eta_k^+ = \sum_{i=1}^{N} g_{ki} c_i^+ + h_{ki} c_i$, then the Hamiltonian becomes

$$H = \sum_{k=1}^{N} \Lambda_k \eta_k^+ \eta_k + \text{const}, \tag{8}$$

two coupled matrix equations satisfy $\phi_k(\boldsymbol{A} - \boldsymbol{B}) = \Lambda_k \psi_k, \psi_k(\boldsymbol{A} + \boldsymbol{B}) = \Lambda_k \phi_k$, where the components of the two column vectors ϕ_{ki}, ψ_{ki} are given by $\phi_{ki} = g_{ki} + h_{ki}, \psi_{ki} = g_{ki} - h_{ki}$. Finally, the ground state of the system $|\psi_0\rangle$ can be written as $\eta_k |\psi_0\rangle = 0$.

Before we talk about the entanglement, let us have a brief review of spin–spin correlation functions. The spin–spin correlation functions for ground state and the average magnetization per spin are defined as[25]

$$\begin{aligned} S_{lm}^x &= \frac{1}{4} \langle \psi_0 | \sigma_l^x \sigma_m^x | \psi_0 \rangle, \\ S_{lm}^y &= \frac{1}{4} \langle \psi_0 | \sigma_l^y \sigma_m^y | \psi_0 \rangle, \\ S_{lm}^z &= \frac{1}{4} \langle \psi_0 | \sigma_l^z \sigma_m^z | \psi_0 \rangle, \\ M_i^z &= \frac{1}{2} \langle \psi_0 | \sigma_i^z | \psi_0 \rangle. \end{aligned}$$

These correlation functions are given as expectation values of products of fermion operators. By using Wick's theorem,[26] the above expressions can be expressed as

$$\boldsymbol{S}_{lm}^x = \frac{1}{4} \begin{pmatrix} G_{l,l+1} & G_{l,l+2} & \cdots & G_{l,m} \\ \vdots & \vdots & \ddots & \vdots \\ G_{m-1,l+1} & G_{m-1,l+1} & \cdots & G_{m-1,m} \end{pmatrix},$$

$$\boldsymbol{S}_{lm}^y = \frac{1}{4} \begin{pmatrix} G_{l+1,l} & G_{l+1,l+1} & \cdots & G_{l+1,m-1} \\ \vdots & \vdots & \ddots & \vdots \\ G_{m,l} & G_{m,l+1} & \cdots & G_{m,m-1} \end{pmatrix}$$

$$S_{lm}^z = \frac{1}{4}(G_{l,l} G_{m,m} - G_{m,l} G_{l,m}),$$

$$M_i^z = \frac{1}{2} G_{i,i},$$

where $G_{i,j} = -\sum_k^N \psi_{ki} \phi_{kj}$.

The concurrence C that can be regarded as a good measure of entanglement for a two-qubit density matrix is defined as[27]

$$C(\boldsymbol{\rho}) = \max(0, \lambda_1 - \lambda_2 - \lambda_3 - \lambda_4), \tag{9}$$

where λ_1, λ_2, λ_3, λ_4 are the eigenvalues of the spin-flipped density operator R in decreasing order, $R = \sqrt{\sqrt{\boldsymbol{\rho}} \tilde{\boldsymbol{\rho}} \sqrt{\boldsymbol{\rho}}}$, where $\tilde{\boldsymbol{\rho}} = (\boldsymbol{\sigma}_y \otimes \boldsymbol{\sigma}_y) \boldsymbol{\rho}^* (\boldsymbol{\sigma}_y \otimes \boldsymbol{\sigma}_y)$, $\tilde{\boldsymbol{\rho}}$ denotes the complex conjugate of $\boldsymbol{\rho}$, $\boldsymbol{\sigma}_y$ is the usual Pauli matrix. Concurrence C ranges from zero to one, the minimal value of the concurrence is zero (in this case two-qubit states are prepared in a separable state), while for any $C > 0$ two qubits are entangled. The maximal value of $C = 1$ corresponds to maximally entangled states that are locally unitary equivalent to Bell states.

The entanglement properties of this state are described by a two-spin reduced density matrix, which can be obtained from the density matrix of the entire system with all the sites but i and j traced out. Using the operator expansion for the density matrix and the symmetries of the Hamiltonian,[28] in the basis states $\{|\uparrow\uparrow\rangle, |\uparrow\downarrow\rangle, |\downarrow\uparrow\rangle, |\downarrow\downarrow\rangle\}$, the density matrix $\boldsymbol{\rho}$ reads

$$\boldsymbol{\rho} = \begin{pmatrix} \rho_{1,1} & 0 & 0 & \rho_{1,4} \\ 0 & \rho_{2,2} & \rho_{2,3} & 0 \\ 0 & \rho_{3,2} & \rho_{3,3} & 0 \\ \rho_{4,1} & 0 & 0 & \rho_{4,4} \end{pmatrix},$$

with

$$\lambda_1 = \sqrt{\rho_{1,1}\rho_{4,4}} + |\rho_{1,4}|, \quad \lambda_2 = \sqrt{\rho_{2,2}\rho_{3,3}} + |\rho_{2,3}|,$$

$$\lambda_3 = \sqrt{\rho_{1,1}\rho_{4,4}} - |\rho_{1,4}|, \quad \lambda_4 = \sqrt{\rho_{2,2}\rho_{3,3}} - |\rho_{2,3}|.$$

We can express all the matrix elements in the density matrix in terms of different spin–spin correlation functions:

$$\begin{aligned} \rho_{1,1} &= \frac{1}{2} M_l^z + \frac{1}{2} M_m^z + S_{lm}^z + \frac{1}{4}, \\ \rho_{2,2} &= \frac{1}{2} M_l^z - \frac{1}{2} M_m^z - S_{lm}^z + \frac{1}{4}, \\ \rho_{3,3} &= \frac{1}{2} M_m^z - \frac{1}{2} M_l^z - S_{lm}^z + \frac{1}{4}, \\ \rho_{4,4} &= -\frac{1}{2} M_l^z - \frac{1}{2} M_m^z + S_{lm}^z + \frac{1}{4}, \\ \rho_{2,3} &= S_{lm}^x + S_{lm}^y, \\ \rho_{1,4} &= S_{lm}^x - S_{lm}^y. \end{aligned}$$

3. Results and discussions

In this paper, our aim is to analyse the dynamics of entanglement in the transverse Ising model by varying the exchange couplings, the external magnetic fields and the system impurity. Increasing interest has been drawn for the role of the ground state entanglement in detecting the quantum phase transitions for various many-body systems, with a maximal next-nearest-neighbouring concurrence at the transition point. First, we examine the change of the entanglement for the next-nearest-neighbouring concurrence $C(i, i+2)$ for different values of the impurity as the parameter λ varies. Figure 1 depicts the next-nearest-neighbouring concurrence $C(49, 51)$ near particular locations of the system for different values of the impurities ζ as a function of the reduced coupling constant λ, with the system size $N = 101$. We can see that as the concurrence increases, a maximum at a critical point λ_c is close to zero and above it. As ζ increases, the concurrence tends to increase faster, the width of the change becomes narrow, and the λ_c, where concurrence approaches maximum, shift to the left very rapidly. We denote the coupling parameter where the first abrupt jump occurs as a characteristic parameter λ_c. In the absence of the impurity ($\zeta = 0$), $\lambda_c = 1$, the maximal value of entanglement is about 4.3×10^{-3}. This is consistent with the result in Ref.[28]. For the parameter $\zeta = 0.1, 0.5, 1.0$, it is evident to observe that increasing the strength of the coupling interaction impurities can enhance the peak of next-nearest-neighbouring concurrence and decreases the characteristic λ_c. When $\zeta = 1.0$, we also see that a maximal next-nearest-neighbouring concurrence at the critical point can arrive at about 23.5×10^{-3}, which is much larger than that in the pure Ising spin chain case. So the coupling interaction impurity is a more efficient control parameter, and more next-nearest-neighbouring entanglement and lower critical transition point can be obtained by adjusting the value of these parameters.

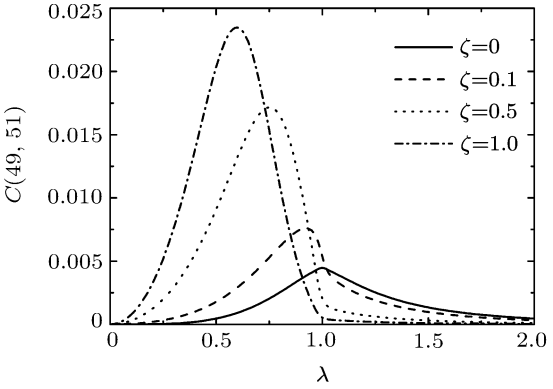


Fig.1. The next-nearest-neighbouring concurrence $C(49, 51)$ as a function of the reduced coupling constant λ for different impurities ζ, $\varepsilon = 0.1$. The system size $N = 101$.

In Fig.2, we show the results of the next-nearest-neighbouring concurrence between sites 49 and 51, as a function of the parameter λ for different strengths of the external magnetic field ξ in the Gaussian distribution. It shows results similar to those obtained in the last subsection, but if we compare Figs.1 and 2 carefully, we can easily find some differences between them. Firstly, different from the effect of the exchange couplings, in Fig.2 the concurrence increases slowly and tends to move to infinity by increasing the value of the parameter ξ. Secondly, although the external magnetic field defect is considered, the entanglement peak between the next-nearest-neighbours increases to only 7×10^{-3}, which is lower than that in Fig.1. Compared with that previously obtained in Ref.[19] with nearest-neighbour entanglement, the numerical calculations show that the nearest-neighbouring concurrence decreases with the increase of ξ for the spin chain, which indicates that the behaviours are very different from those in Fig.2. That is to say, the entanglement peak between the next-nearest-neighbours increases to a larger value once the defect is introduced. The strong ξ is helpful to keep better next-nearest-neighbouring entanglement and decrease nearest-neighbouring entanglement for the defect distribution of the external magnetic field.

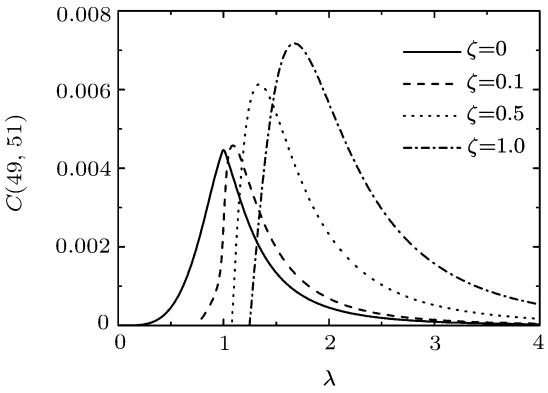


Fig.2. The next-nearest-neighbouring concurrence $C(49, 51)$ as a function of the parameter λ for different strengths of the external magnetic field ξ, with $\varepsilon = 0.1$. The system size is $N = 101$.

Up to now we have examined the next-nearest-neighbouring concurrence $C(49, 51)$ with different

strengths of the exchange couplings and the magnetic field impurities. From Figs.1 and 2, one can see that in the analysis the above parameters play an important role in enhancing entanglement. In contrast to previous investigations, where we focus on the effect of the defect strength on the concurrence at a fixed width, in the present section, keeping a fixed strength, we focus on the role of the defects distribution width in the concurrence. To study the effect of the defects distribution width on the entanglement is thus necessary and important. A similar analysis can be carried out for the next-nearest-neighbouring concurrence $C(49,51)$. This is demonstrated in Figs.3 and 4, which show the change of the concurrence with the distribution width. From Fig.3, we can see that the entanglement can be modified by varying the width of the defect distribution ε for a fixed strength ($\zeta = 1$). In our calculation, we find that the concurrence tends to increase and the curves of the $C(49,51)$ shift monotonously to the right by increasing the distribution width of the impurity to a fixed strength. Moreover, the maximum of $C(49,51)$ tends to increase at first and then decrease with increasing λ, in other words, the maximum entanglement can be enhanced by introducing a properly disordered distribution width. Another question is how the magnetic field defect distribution width ε affects the entanglement between the next-nearest-neighbours. Compared with the effect of controlling the exchange couplings defect distribution width, in Fig.4, the curves $C(49,51)$ for different magnetic defect distribution width are plotted. The peak of the maximal entanglement becomes weak compared with the case in Fig.3, it is the different defect distribution width that leads to considerable different evolution of the entanglement. For a fixed strength of the magnetic field defects ($\xi = 1$), we see that the maximum of $C(49,51)$ tends to increase monotonously due to increasing magnetic field disordered distribution width for a fixed strength. Moreover, the concurrence tends to increase faster and the curves of the $C(49,51)$ shift monotonously to the left. However, for a fixed width of magnetic field defects, the concurrence tends to increase and the curves of the $C(49,51)$ shift monotonously to the right due to the increasing strength of magnetic field defects.

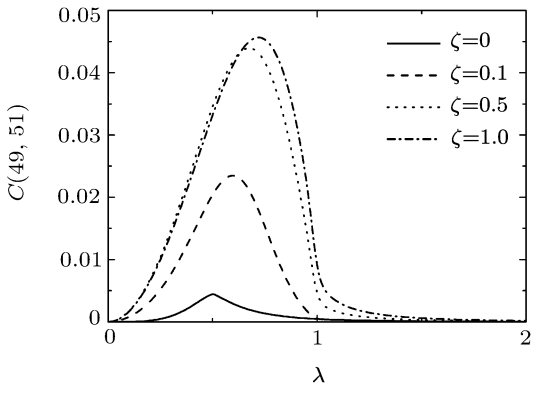


Fig.3. The next-nearest-neighbouring concurrence $C(49,51)$ as a function of the reduced coupling constant λ for different values of the width of the distribution ϵ with $\zeta = 1.0$. The system size $N = 101$.

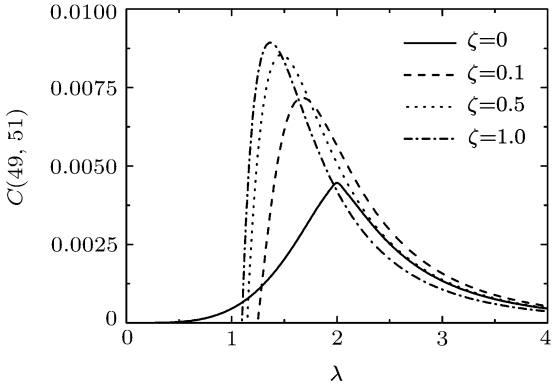


Fig.4. The next-nearest-neighbouring concurrence $C(49,51)$ as a function of the reduced coupling constant λ for different values of the width of the distribution ϵ with $\xi = 1.0$. The system size $N = 101$.

4. Conclusions

To summarize, the ground next-nearest-neighbouring entanglement near particular locations in a 1D $s = 1/2$ random Ising spin system has been investigated. Through analysing the exchange couplings and external magnetic fields with defects, we have discussed how to manipulate a spin chain with local control of the strengths of exchange couplings and the magnetic field defects, as well as the defects distribution width, showing that the entanglement can be remotely controlled, and that entanglement can be adjusted to a large extent in order to achieve the desired next-nearest-neighbouring entanglement. One possibility to implement this model in a realistic setup is to arrange spin chains with atoms in an optical lattice. The defects of exchange couplings or external magnetic fields should enable the control of next-nearest-neighbouring entanglement and quantum phase transition.

References

[1] Bennett C H, Brassard G, Crépeau C, Jozsa R, Peres A and Wootters W K 1993 *Phys. Rev. Lett.* **70** 1895

[2] Wei H, Deng Z J, Zhang X L and Feng M 2007 *Phys. Rev.* A **76** 054304

[3] Cheng W W, Huang Y X, Liu T K and Li H 2007 *Chin. Phys.* **16** 38

[4] Grover L 1998 *Phys. Rev. Lett.* **80** 4329

[5] Wu Y and Machta J 2005 *Phys. Rev. Lett.* **95** 137208

[6] Wang X G 2001 *Phys. Rev.* A **64** 012313
Wang X G 2002 *Phys. Rev.* A **66** 044305
Wang X G 2002 *Phys. Rev.* A **66** 034302

[7] Asoudeh M and Karimipour V 2005 *Phys. Rev.* A **71** 022308

[8] Zhang G F and Li S S 2005 *Phys. Rev.* A **72** 034302
Zhou L, Song H S, Guo Y Q and Li C 2003 *Phys. Rev.* A **68** 024301

[9] Kargarian M, Jafari R and Langari A 2008 *Phys. Rev.* A **77** 032346
Li D C and Cao Z L 2008 *Eur. Phys. J.* D **50** 207

[10] Lidar D A, Bacon D and Whaley K B 1999 *Phys. Rev. Lett.* **82** 4556

[11] Werner P, Vloker K, Troyer M and Chakravarty S 2005 *Phys. Rev. Lett.* **94** 047201

[12] Furman G B, Meerovich V M and Sokolovsky V L 2008 *Phys. Rev.* A **77** 062330

[13] de Oliveira T R, Rigolin G, de Oliveira M C and Miranda E 2006 *Phys. Rev. Lett.* **97** 170401

[14] Wei T C, Das D, Mukhopadyay S, Wisheshwera S and Goldbart P 2008 *Phys. Rev.* A **77** 062330

[15] Yang M F 2005 *Phys. Rev.* A **71** 030302(R)

[16] Zhu S L 2006 *Phys. Rev. Lett.* **96** 077206

[17] Garnerone S, Jacobson N T, Haas S and Zanardi P 2009 *Phys. Rev. Lett.* **102** 057205

[18] Osterloh A, Amico L, Falci G and Fazio R 2002 *Nature* **416** 608

[19] Huang Z, Osenda O and Kais S 2004 *Phys. Lett.* A **322** 137

[20] Osenda O, Huang Z and Kais S 2003 *Phys. Rev.* A **67** 062321

[21] Shan C J, Cheng W W, Liu T K, Huang Y X and Li H 2008 *Chin. Phys.* B **17** 4002
Shan C J, Cheng W W, Liu T K, Huang Y X and Li H 2008 *Chin. Phys.* B **17** 0794
Shan C J, Cheng W W, Liu T K, Huang Y X and Li H 2008 *Chin. Phys. Lett.* **25** 817

[22] Venuti L C, Giampaolo S M, Illuminati F and Zanardi P 2007 *Phys. Rev.* A **76** 052328

[23] Venuti L C, Esposti Boschi C D and Roncaglia M 2007 *Phys. Rev. Lett.* **99** 060401

[24] Jordan P and Wigner E 1928 *Z. Phys.* **47** 631

[25] Lieb E, Schultz T and Mattis D 1961 *Ann. Phys.* **60** 407

[26] Wick G C 1950 *Phys. Rev.* **80** 268

[27] Wooters W K 1998 *Phys. Rev. Lett.* **80** 2245

[28] Osborne T J and Nielsen M A 2002 *Phys. Rev.* A **66** 032110